Springer

KSME

Journal of Mechanical Science and Technology 24 (2010) 231~235
www.springerlink.com/content/1738-494x
DOI 10.1007/s12206-009-1133-6

Design of magnetically levitated rotors in a large flywheel energy storage system from a stability standpoint

Seong-yeol Yoo[1], Wook-ryun Lee[2], Yong-chae Bae[2] and Myounggyu Noh[1,*]

[1]*Division of Mechatronics Engineering, Chungnam National University, Daejeon, 305-764, Korea*
[2]*Korea Electric Power Research Institute, Daejeon, Korea*

(Manuscript Received May 1, 2009; Revised September 26, 2009; Accepted October 16, 2009)

Abstract

The stability of flywheels in an energy storage system supported by active magnetic bearings (AMBs) is studied in this paper. We designed and built two flywheel energy storage systems (FESS) that can store up to 5 kWh of usable energy at a maximum speed of 18,000 rpm. One is optimized to store as much energy as possible, resulting in a flywheel with a strong gyroscopic coupling. The other has a much smaller gyroscopic coupling for ease of control. To analyze the stability of the system accurately, we derived the dynamic models of the rotor using finite-element method and integrated them with the models of the bearings, amplifiers, and sensors to obtain the simulation model of the system. We validated the model through experiments and compared the stability of these two systems.

Keywords: Flywheel energy storage system; Active magnetic bearing; Stability; Flexible rotor model; Reduced-order model

1. Introduction

Flywheel energy storage systems (FESS) store electric energy in terms of the kinetic energy of a rotating flywheel, and convert this kinetic energy into electric energy when necessary. A FESS is a viable technology for energy storage because it is environmentally safe, can sustain infinite charge/discharge cycles, and has higher power-to-weight ratio than chemical batteries [1]. FESSs commonly use active magnetic bearings (AMBs) for contact-free operation to maximize the efficiency of the system.

The energy storage capacity of a FESS is proportional to the principal mass-moment of inertia I_p and the square of the running speed Ω. The energy capacity is independent of the transverse mass-moment of inertia I_t. Therefore, if we only consider the aspect of the energy storage, a radially thick flywheel (larger I_p / I_t ratio) is advantageous over a slender flywheel (smaller I_p / I_t ratio). However, the gyroscopic moment of a radially thick flywheel is bigger than that of a slender flywheel, which could make the system unstable.

Many researchers have investigated flywheel systems using flexible rotor modeling in recent years. Hawkins, et al. [2] studied the controller design and modeling for large capacity flywheel systems with AMBs. Ahn, et al. [3], Jeon, et al. [4], and Lei, et al. [5] investigated the modeling of a flexible rotor with AMBs. Mohiuddin, et al. [6] applied reduced order modeling for flexible rotor-bearing systems.

In this paper, we designed and built two flywheel systems. One is optimized to store as much energy as possible, while the other has a much smaller gyroscopic coupling for ease of control. To analyze accurately the stability of the system, we derived the dynamic models of the rotor using finite-element method and modal truncation. The rotor model is integrated with the models of AMBs, amplifiers, and sensors to obtain the simulation model of the system. This model is validated with the experimentally obtained system responses. Finally, we compared the stability of the two systems using the sensitivity functions and pole locations of the closed-loop transfer functions.

2. System description

The two flywheel systems considered in this paper are shown in Fig. 1. The flywheels are made from multi-layer fiber-reinforced composites and are fitted to metal rotors through aluminum hubs. The rotors are supported by a set of two radial AMBs and a thrust AMB. As AMBs are open-loop unstable, a set of five non-contact position sensors detects the position of the rotor so that the feedback controller can adjust the coil currents of AMBs to maintain contact-free operation. The radial AMBs in FESS-II have slightly bigger capacity to counteract the increased mass. A motor/generator is located

† This paper was presented at the ICMDT 2009, Jeju, Korea, June 2009. This paper was recommended for publication in revised form by Guest Editors Sung-Lim Ko, Keiichi Watanuki.

*Corresponding author. Tel.: +82 42 821 6877, Fax.: +82 42 823 4919
E-mail address: mnoh@cnu.ac.kr

either below or above the flywheels. These two systems are designed to store the same 5 kWh of usable energy at the same operating speed of 18,000 rpm in a vacuum environment. Table 1. compares several parameters of these two systems.

3. System modeling

3.1 Rotor model

To describe accurately the dynamic behavior of the rotor, we used a flexible rotor model based on finite element methods [7]. This dynamic model can be written as,

$$\begin{bmatrix}\mathbf{M} & \mathbf{0}\\ \mathbf{0} & \mathbf{M}\end{bmatrix}\begin{bmatrix}\ddot{\mathbf{w}}_x\\ \ddot{\mathbf{w}}_y\end{bmatrix}+\begin{bmatrix}\mathbf{0} & \Omega\mathbf{G}\\ -\Omega\mathbf{G} & \mathbf{0}\end{bmatrix}\begin{bmatrix}\dot{\mathbf{w}}_x\\ \dot{\mathbf{w}}_y\end{bmatrix}+\begin{bmatrix}\mathbf{K} & \mathbf{0}\\ \mathbf{0} & \mathbf{K}\end{bmatrix}\begin{bmatrix}\mathbf{w}_x\\ \mathbf{w}_y\end{bmatrix}=\begin{bmatrix}\mathbf{F}_x\\ \mathbf{F}_y\end{bmatrix} \tag{1}$$

where $\mathbf{w}_x$ and $\mathbf{w}_y$ are the nodal displacements in the radial planes, and $\mathbf{M}$, $\mathbf{G}$, and $\mathbf{K}$ are the mass, gyroscopic, and stiffness matrices, respectively. The gyroscopic effect results in dynamics dependent on running speed Ω. The bearing forces and disturbances enter into the dynamics through $\mathbf{F}_x$ and $\mathbf{F}_y$.

Typically, the size of the dynamic model (1) is quite large, which makes it difficult to adequately design controllers using this model. Further, dynamic modes much higher than the maximum operating speed may contribute negligibly to the overall dynamics. To describe the flexible dynamics of the rotor in the frequency range of interest, we can use modal truncation [8] to obtain a reduced-order model. Modal truncation starts by obtaining mass normalized mode shape vectors Φ that satisfy the following:

$$\Phi^T\mathbf{M}\Phi=\mathbf{I}$$
$$\Phi^T\mathbf{K}\Phi=\Lambda^2 \tag{2}$$

where Λ is a diagonal matrix, the elements of which are the natural frequencies. If we partition the mode shapes into *master* and *slave* modes as

$$\Phi=[\Phi_m\ \ \Phi_s] \tag{3}$$

and approximate that

$$\mathbf{w}_x=\Phi\xi=\begin{bmatrix}\Phi_m & \Phi_s\end{bmatrix}\begin{bmatrix}\xi_m\\ \xi_s\end{bmatrix}\approx\Phi_m\xi_m \tag{4}$$

$$\mathbf{w}_y=\Phi\psi=\begin{bmatrix}\Phi_m & \Phi_s\end{bmatrix}\begin{bmatrix}\psi_m\\ \psi_s\end{bmatrix}\approx\Phi_m\psi_m \tag{5}$$

the dynamic model (1) can be reduced to

$$\begin{bmatrix}\ddot{\xi}_m\\ \ddot{\psi}_m\end{bmatrix}+\begin{bmatrix}\mathbf{0} & \Omega\Phi_m^t\mathbf{G}\Phi_m\\ -\Omega\Phi_m^t\mathbf{G}\Phi_m & \mathbf{0}\end{bmatrix}\begin{bmatrix}\dot{\xi}_m\\ \dot{\psi}_m\end{bmatrix}+\begin{bmatrix}\Lambda^2 & \mathbf{0}\\ \mathbf{0} & \Lambda^2\end{bmatrix}\begin{bmatrix}\xi_m\\ \psi_m\end{bmatrix}=\begin{bmatrix}\Phi_m^t\mathbf{F}_x\\ \Phi_m^t\mathbf{F}_y\end{bmatrix} \tag{6}$$

Table 1. Parameters of of FESS-I and FESS-II systems.

Specifications	FESS-I	FESS-II
Mass (kg)	235	400
Polar moment of inertia (kg-m^2)	13.2	13.6
Transverse moment of inertia (kg-m^2)	9.4	27.1
Axial length of the rotor (mm)	778	1147
Flywheel diameter (mm)	716	580
Load capacity of radial AMB (N)	1008	1370
Axial length of radial AMB (mm)	55	55

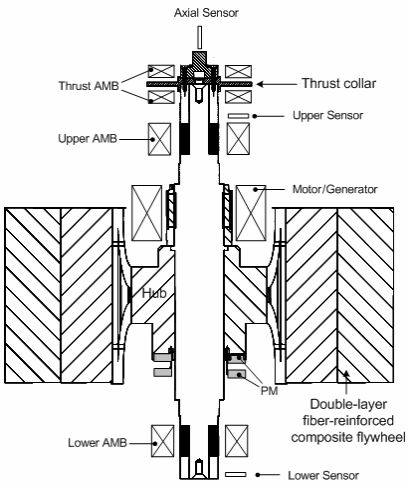

(a) FESS-I

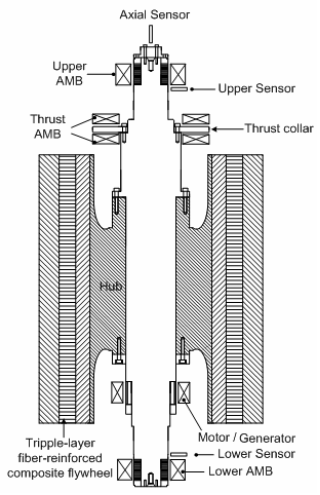

(b) FESS-II

Fig. 1. A schematic view of two types of flywheel energy storage systems.

3.2 Radial AMB model

The force produced by a radial AMB is related to the coil currents in a nonlinear fashion. If a bias force is maintained to guarantee a finite force slew rate, the force is also affected by the radial position of the rotor. Using the bias linearization method [9], the bearing force can be linearized with respect to the coil currents and rotor position. This linear relationship can be expressed as

$$F_q^A = -K_r^A q + K_i^A i_q, \quad A = U, L \text{ and } q = x, y \tag{7}$$

where K_r^U and K_r^L are the radial stiffness of the upper and lower radial AMBs, respectively. In Eq. (7), K_i^U and K_i^L are the actuator gains of the upper and lower radial AMBs, respectively.

3.3 Controller model

As radial AMBs are open-loop unstable, a feedback controller is necessary for stable levitation. Typically, a proportional-derivative (PD) controller is used for this purpose. The transfer function of a PD controller with the proportional gain of K_p and the derivative gain of K_d can be written as follows:

$$G_c(s) = K_p + K_d s \tag{8}$$

The problem with this PD controller is that the gain increases unboundedly with respect to the frequency. If we limit the high-frequency gain by introducing a bandwidth to the controller, the transfer function is modified to

$$G_c(s) = K_p + \frac{K_d s}{\tau_d s + 1} \tag{9}$$

where τ_d defines the bandwidth.

For the system FESS-I with a strong gyroscopic effect, the controller can be further modified to include cross-feedback [10].

3.4 System model

The aforementioned models can be put together to construct a system model. The actual system includes the power amplifiers that generate coil currents corresponding to the controller output. The system also has position sensors that detect the radial position of the rotor. The block diagram of the system model is shown in Fig. 2. Signal *d* is the input disturbance, which represents an unbalance force. The system may have another disturbance in terms of sensor noise that will be added to the sensor output.

4. Model validations

To check the validity of the model we derived, we carried out system identification experiments for both systems. The procedure of the experiments begins by first injecting swept-sine signals as the disturbance input *d,* shown in Fig. 2, and measuring the sensor outputs while maintaining the levitation of the rotors.

Figs. 3 and 4 show the experimental results compared with the identified models. Except for some discrepancies at the low frequency region, the system models derived from full-scale FEM rotor models (full-order models) match well with the experimental observations for the systems FESS-I and FESS-II. The reduced-order models are constructed in such a

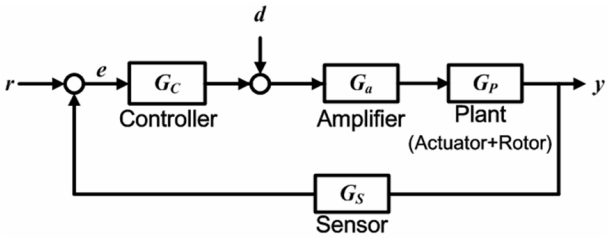

Fig. 2. Block diagram of the system model.

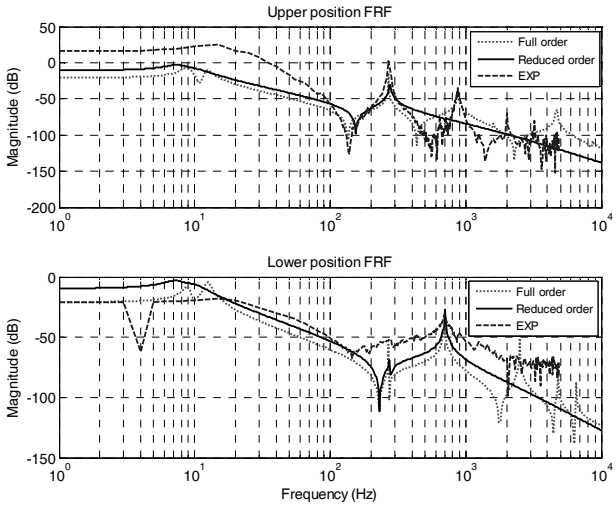

Fig. 3. Model identification results for FESS-I.

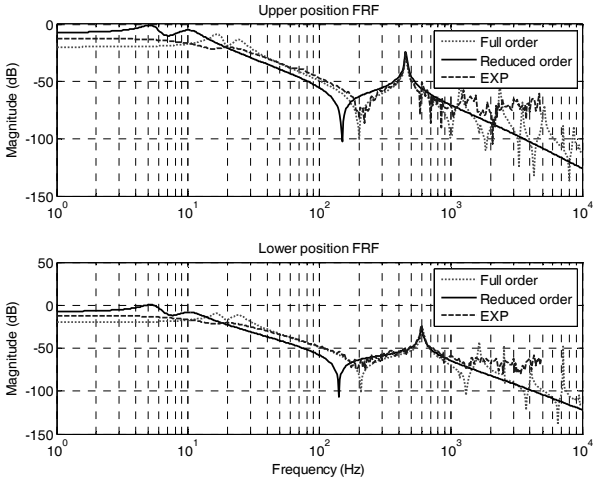

Fig. 4. Model identification results for FESS-II.

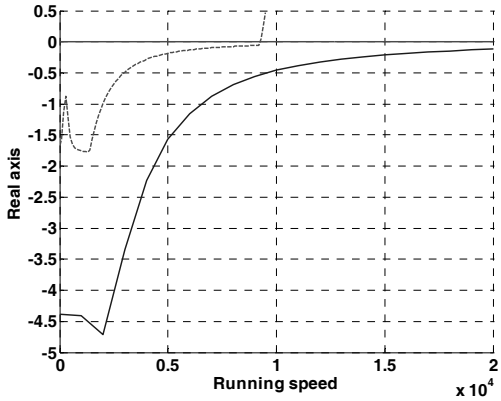

Fig. 5. Real part of the rightmost poles of FESS-I (dotted line) and FESS-II (solid line).

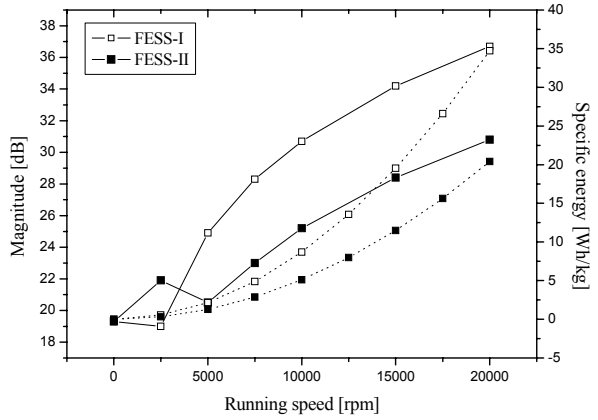

Fig. 6. Peak sensitivities (solid lines) of FESS-I and FESS-II with respect to the running speed as well as the corresponding specific energy (dotted lines).

way as to include only the first bending modes of the rotors. As expected, the reduced-order models correctly predict the frequency responses up to the first bending modes.

5. Stability analysis

A direct way of checking system stability is to look at the pole locations of the closed-loop transfer functions. If the poles stay on the left half of the complex plane, the system is stable. Fig. 5 shows the real parts of the right-most poles of FESS-I and FESS-II systems. If the real part becomes positive, this means the system is unstable. As the dynamics of the flywheel is dependent on the running speed, the poles move with respect to the speed. A radially thick flywheel system, FESS-I, becomes unstable at around 9,000 rpm, which is consistent with the experimental observations. In contrast, FESS-II stays stable even at 20,000 rpm. It should be noted that the controller gains of the two systems are kept at the same values for comparison. The controller gains for FESS-I system can be adjusted to guarantee stability in the operating speed range. The results in Fig. 5 mean that FESS-I is less stable than FESS-II with the same controller.

Even if the system is stable, the system may be susceptible to the disturbances if the poles stay close to the imaginary axis of the complex plane. The sensitivity function can conveniently be used to quantify how much the system is susceptible to the disturbances. Referring to the block diagram in Fig. 2, the sensitivity function T_s is defined as follows:

$$e = T_s r \quad . \tag{10}$$

The larger the magnitude of the sensitivity, the more susceptible the system is to the disturbances.

Fig. 6 shows the peak sensitivities $\|T_s(j\omega)\|_\infty$ of FESS-I and FESS-II (solid lines). The system FESS-I has higher sensitivity peaks than FESS-II except at very low speeds. Fig. 6 also demonstrates how much FESS-I is better than FESS-II in terms of specific energy, which is the stored energy per unit mass. As the mass of FESS-I is only 60% of FESS-II, the specific energy of FESS-I is more than 70% higher than that of FESS-II. Therefore, FESS with a larger I_p / I_t ratio is preferable to the one with a smaller inertia ratio. However, the results of this paper elucidate that one must consider not only the energy capacity but also the stability of the system when designing a FESS supported by AMBs.

References

[1] N. Koshizuka, et al., Present status of R & D on superconducting magnetic bearing technologies for flywheel energy storage system, *Physica C-Superconductivity and Its Applications* 378 (2002) 11-17.

[2] L. A. Hawkins, B. T. Murphy and J. Kajs, Analysis and testing of a magnetic bearing energy storage flywheel with gain-scheduled, MIMO control, *Proc. ASME Turboexpo* (2000).

[3] H. J. Ahn and D. C. Han, System modeling and robust control of an AMB spindle : Part I modeling and validation for robust control, *KSME Int. Journal* 17 (12) (2003) 1844-1854.

[4] S. Jeon, H. J. Ahn and D. C. Han, Model validation and controller design for vibration suppression of flexible rotor using AMB, *KSME Int. Journal* 16 (12) (2002) 1583-1593.

[5] S. Lei and A. Palazzolo, Control of flexible rotor systems with active magnetic bearings, *Journal of Sound and Vibration* 314 (2008) 19-38.

[6] M. A. Mohiuddin, M. Bettayeb and Y. A. Khulief, Dynamic analysis and reduced order modelling of flexible rotor-bearing systems, *Computers & Structures* 69 (3) (1998) 349-359.

[7] H. D. Nelson and J. M. McVaugh, The dynamics of rotor-bearing systems using finite elements, *ASME Journal of Eng. For Ind.* 98 (1976) 593-600.

[8] D. Childs, *Turbomachinery Rotordynamics*, John Wiley & Sons, New York, USA (1993).

[9] E. H. Maslen and D. C. Meeker, Fault tolerance of magnetic bearings by generalized bias current linearization, *IEEE Trans. Magnetics* 31 (1995) 2304-2314.

[10] M. Ahrens, L. Kucera and R. Larsonneur, Performance of a magnetically suspended flywheel energy storage device, *IEEE Trans. Control Sys. Tech.* 4 (5) (1996) 494-502.

Seong-Yeol Yoo received his M.S. degree in mechatronics engineering in 2007 from Chungnam National University, Korea, where he is currently a Ph.D candidate in the Department of Mechatronics Engineering. His research interests are in the fields of actuators, rotor-dynamics, and low/zero-power control of AMBs.

Myounggyu Noh received his Ph.D in mechanical engineering from the University of Virginia, U.S.A., in 1996. Since 1999, he has been with Chungnam National University, Korea, and is currently a professor. His research interest includes magnetic suspension systems, intelligent sensors and actuators, and biomedical applications.